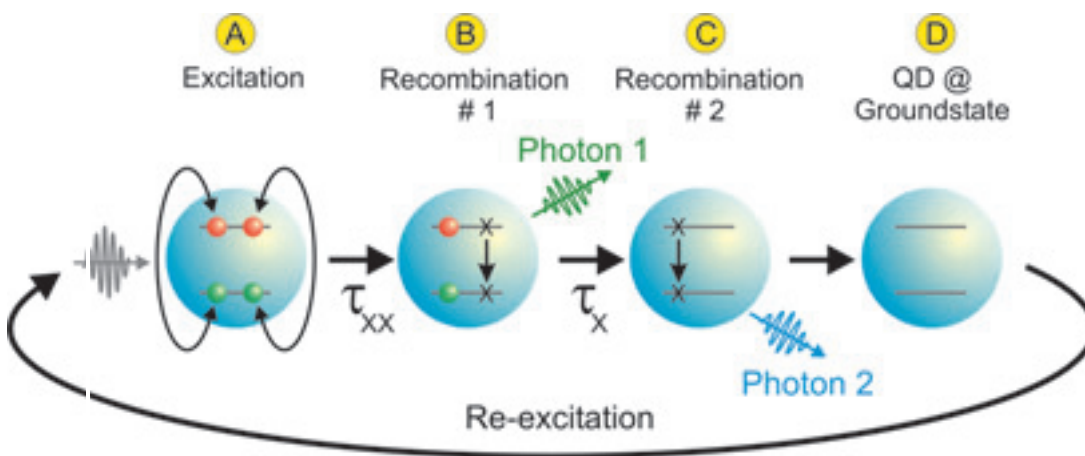


# Semiconductor single-photon sources

A single photon source, which is able to generate photons on demand allows the ultimate quantum control of the photon generation process, i.e., single photons can be generated within short time intervals with a deterministic dwell time between successive photon generation events. Such a source has the potential of enabling many new applications in the field of photonics and quantum information technology. This is in particular true for quantum cryptography, which exploits the fundamental principles of quantum mechanics to provide unconditional security for communication. An essential element of secure key distribution in quantum cryptography is an optical source emitting a train of pulses that each contain one and only one photon. Because measurements unavoidably modify the state of a single quantum system, an eavesdropper cannot gather information

about the secret key without being noticed, provided that the pulses used in transmission do not contain two or more photons. Recently, it has also been shown that the availability of a single-photon source which is able to generate indistinguishable photons enables the implementation of quantum computation using only linear optical elements and single photon detectors. Possible other applications are imaging and lithography beyond the diffraction limit as well as quantum teleportation.



about the secret key without being noticed, provided that the pulses used in transmission do not contain two or more photons. Recently, it has also been shown that the availability of a single-photon source which is able to generate indistinguishable photons enables the implementation of quantum computation using only linear optical elements and single photon detectors. Possible other applications are imaging and lithography beyond the diffraction limit as well as quantum teleportation.

## 1. Introduction

The single-photon sources used today either employ highly attenuated laser pulses or rely on parametric down-conversion. Both schemes possess a serious disadvantage since photons are created randomly, i.e., with a Poissonian photon statistics. In order to maintain a low multi-photon emission probability the average photon number per pulse has to be kept as low as  $\sim 0.1$ . The realization of a practical single photon source requires three main elements: a single quantum emitter, regulation of the excitation and/or the recombination process and an efficient output coupling of the single photons. The active emitter should possess a short radiative recombination time to allow operation at high repetition rates. Furthermore, the possibility of electrical pumping is desirable with respect to a compact and robust source.

Though working until now at low temperature, epitaxially self-assembled InAs quantum dots (QDs) are ideal candidates since they offer several advantages, including high quantum efficiencies of  $\eta \sim 1$ , large dipole moments, narrow linewidths that can be close to the Fourier-transform limit, and the option of electrical pumping. The triggered single-photon emission at the single exciton ground state transition of a self-assembled QD is ensured by a *pulsed excitation*, the *anharmonicity* of the multi-exciton spectrum in combination with *slow relaxation* of highly excited QD states. Spontaneous emission of a quantum emitter is generally emitted in all directions (full solid angle) and therefore hard to capture efficiently. For a practical use, however, the emitter should be coupled to a cavity mode with a directional field profile. Self-assembled QDs can be easily embedded into an appropriate microcavity, e.g., into a micro-pillar. This allows an efficient collection of the single photons thus enabling their use for external applications.

In the following, we will first give an introduction to the physics of quantum dots and the concept of photon statistics measurements. Second, we will discuss recent experimental results where resonant coupling of the QD transitions to a cavity mode has been achieved. Efficient triggered generation of single and photon-pair emission is demonstrated. Finally, the

remaining challenges for the use of QD pillar cavities as single photon sources will be discussed.

## 2. Quantum Dots

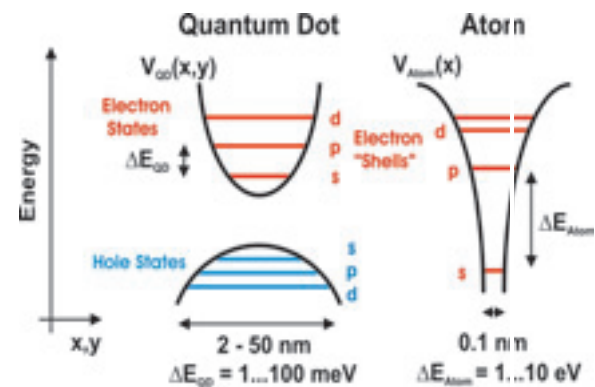
Semiconductor-based QDs typically contain only a few  $10^4$ – $10^5$  atoms of a material *A* (e.g., indium arsenide *InAs*) providing a smaller band gap energy than the surrounding semiconductor matrix material *B* (e.g., (aluminium) gallium arsenide (*AlGaAs*)). During the last two decades, various sophisticated semiconductor growth methods have been developed and refined in order to gain a high degree of control on the exact size and composition of these nanostructures which allows for an application-oriented design. One of the well established methods for self-assembled growth is e.g., the strain-induced Stranskii-Krastanov growth mode in which the formation of islands is achieved via surface energy minimization of droplets of a low band gap material *A* on top of material *B*. Finally, the islands are overgrown by material *B* thus generating a fully embedded QD in the host material *B*.

From a basic energetic view, carriers inside a QD will therefore be subject to a full three-dimensional barrier potential thus trapping these particles. The strong three dimensional confinement leads to quantization effects on the eigenstates of electrons and holes. As a result, a few discrete bound energy eigenstates with limited degeneracy are available for occupation by carriers – which reflects itself in the sharp emission spectra of *single* QDs by a pairwise radiative recombination of electrons and holes from conduction and valence band states, respectively.

## SUMMARY

Exploiting the quantum properties of the light which is emitted from semiconductor nano-structures has the potential of enabling many new applications in the field of photonics and quantum information technology, such as secure communication, imaging and lithography techniques beyond the diffraction limit, as well as photonic quantum computing. Many of these applications require a single-photon source, which is able to generate photons on demand. A single semiconductor quantum dot embedded into a microcavity is able to deliver triggered single photons with ultra-high repetition rates of  $\sim 1$  GHz.

This contribution gives an introduction into the exciting physics of single semiconductor nanostructures and their use as non-classical light sources. The efficient triggered generation of single photons and photon pairs by placing an individual quantum dot into a micropillar cavity is demonstrated. Furthermore, the remaining challenges for the application of quantum dots in pillar cavities as practical single-photon sources will be discussed.



Comparison between basic properties of quantum dots (“artificial atoms”) and real atoms. Both model systems provide discrete bound eigenstates for electrons (atom) or electrons and holes (QD). Due to the significant differences in size, the quasi-harmonic energy splittings between QD shells are on the meV scale ( $\sim 100$  times less than for real atoms).

Even though QDs are often referred to as “artificial atoms” due to these unique characteristics similar to “real” atoms, one should note the differences between these two model systems (01): Due to the small

size of real atoms ( $\sim 0.1$  nm), the anharmonic  $s$ -,  $p$ -,  $d$ -shell structure of eigenstates reveals a high energetic splitting  $\Delta E$  in the 1–10 eV range whereas the quasi-equidistant splitting of QD shells is significantly lower ( $< 100$  meV) due to their comparably large extent (see above). As a direct consequence of this, the emission properties of QDs are sensitive to the lattice temperature in a sense that bound carriers might be thermally activated into unbound states of the barrier material. Experiments on these structures are therefore mainly

done at cryogenic temperatures ( $T < 100$  K). However, progress in high temperature operation of QDs has been already achieved [1] and room temperature operation seems to be possible with specially designed QDs in the near future.

For the generation of radiative quantum cascades, the QDs are excited with short optical or electrical pulses to generate the electron-hole pairs in the barriers (material B) of the QDs. The carriers are subsequently captured by the QDs and relax to the lowest energy levels ( $s$ -shell) within a few tens of picoseconds. Inside a QD, Coulomb interaction between a captured  $s$ -shell electron-hole pair naturally forms the lowest-energy exciton ( $X$ ) state of an excited QD. The scenario of fully occupied  $s$ -shells by two electrons and holes, respectively, represents a biexcitonic ( $XX$ ) configuration. The radiative recombination of this multiexcitonic state occurs in cascaded processes (02), i.e., in sequential optical transitions of the biexciton ( $XX$ ) and the exciton state ( $X$ ). Due to Coulomb

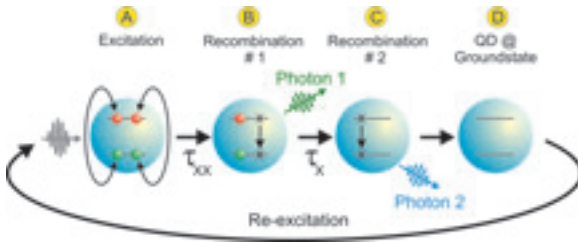
interactions enhanced by strong carrier confinement, the energy of the emitted photons depends sensitively on the number of  $e$ - $h$  pairs that exist inside the QD. If the recombination times of the multiexcitonic states are longer than the recombination time of the free electron-hole pairs in the barriers, each excitation pulse can lead to at most one photon emission event at the corresponding dot transition.

Therefore, a regulation of photon emission processes can be achieved due to a combination of Coulomb interactions creating an anharmonic multiexciton spectrum and vanishing re-excitation probability on short time scales after the corresponding photon emission event at the  $XX$  or  $X$  transitions. Thus, specific photons from the cascade process, e.g., the  $XX$  and  $X$ , can be spectrally filtered out and used to generate single photons or correlated photon pairs. Even the generation of polarization-entangled photons is expected.

### 3. Photon statistics measurements

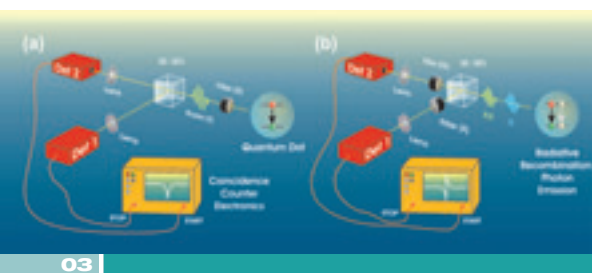
To get insight into the statistical nature of light emitted by the single QD a Hanbury-Brown & Twiss photon-correlation setup was used as is depicted schematically in (03). The basic version (a) of such an experiment consists of two orthogonal detector arms on which the collected photon stream is divided by a 50/50 beam splitter: A narrow band spectral filter is used in front of the HBT setup to select the desired recombination line (e.g., excitonic  $X$  or biexcitonic  $XX$ ) and to reject background light. Due to the quantum mechanical picture of a single photon as an indivisible “wave packet”, each photon can either be detected on one of the two high-sensitivity avalanche photo diodes (Det 1 + Det 2).

If we recall the simple atomistic picture explained in the preceding paragraphs (02), it becomes obvious that immediately after recombination of an  $e$ - $h$  pair (i.e., the emission of a photon of equivalent energy) it is impossible to detect a second identical photon from the same decay process as the initial configuration of  $e$ - $h$  pairs within the QD needs to be re-established first. This argument holds for both continuous wave (cw) and pulsed excitation of the QD. In the case of an ideal single-photon



02

Simplified scenario for the sequential decay of different ( $s$ -shell) electron-hole pair configurations within a single QD forming a photon cascade. After initial excitation of the biexcitonic state  $XX$ , radiative recombination of the first  $e$ - $h$  pair emits a specific photon (#1) thus leaving the QD in its excitonic  $s$ -state (i.e., one  $e$ - $h$  pair in the lowest shell). A second photon (#2) is the result of the sequential decay of the remaining state.  $\tau_{XX}$  ( $\tau_X$ ) represent the radiative lifetimes of the corresponding QD carrier configurations.



03

Photon correlation setup scheme: (a) Auto-correlation: Light collected from the sample (02) is spectrally pre-filtered to select a single narrow QD luminescence decay line. Dividing this photon stream into two 50:50 single-photon detection paths, the statistics of two-photon coincidences separated by a delay  $\tau = t_{\text{stop}} - t_{\text{start}}$  between both detections is investigated. The characteristic behaviour of a single photon source is the so-called “anti-bunching” reflected by a significant dip in the statistics at zero delay ( $\tau = 0$ ); (b) Cross-correlation: Photonic cascades are verified by use of consecutive photons (e.g.  $XX \rightarrow X \rightarrow 0$ ) which – due to their different energy – are spectrally separated within the START and STOP detection arms of the setup. Photonic cascades reflect in a significant antibunching-bunching correlation trace asymmetry (see schematic trace).

emitter (a single QD) the auto-correlation statistics (03a) reveals full suppression of photon pair coincidence events with zero delay, thus reflecting in either (a) correlation trace “dip” at  $\tau=0$  (cw) or (b) the suppression of only the  $\tau=0$  correlation peak within a train of coincidence peaks at integer multiples of the laser pulse period (see also next chapter). In other words, the probability to simultaneously detect two photons from the same decay channel on both detector arms completely vanishes. This *non-classical* behaviour of emission is known as “*photon anti-bunching*” which allows for a clear identification of an atom-like photon source.

(03b) displays the experimental scheme for the identification of temporally correlated two-colour photon pairs from consecutive e-h recombination within a single QD. The basic idea of this *cross-correlation* type of experiment is to prove the *temporal interconnection* between different recombination channels which can be spectrally distinguished.

(02) sketches the main sequence of recombination processes which form such a two-photon cascade. Assuming the lowest energy levels of electrons and holes (s-shell) to be initially occupied by two carriers each, the QD is in its “biexcitonic” (XX) configuration (A). The spontaneous radiative decay of one of the two e-h pairs (transition  $B \rightarrow C$ ) leads to the emission of a characteristic single XX photon which is spectrally selected for detection by only one arm (START) of the correlation setup. Due to the Coulomb interaction (attractive or repulsive, depending on the microscopic conditions of the 3-D carrier confinement of the QD) the decay of the remaining excitonic (X) dot configuration ( $C \rightarrow D$ ) deviates in energy. If the excitation conditions are carefully chosen such that re-excitation in between XX and X decays can be neglected, each spontaneous biexciton recombination should involve the subsequent decay of a remaining exciton thus leaving the QD in its empty state (D). Therefore, in cross-correlation experiments, the second detection arm (STOP channel) of the setup is energetically tuned to the X transition so that in total the distribution  $g^{(2)}(\tau)$  (“second-order correlation function”) of coincidence events between both channels reflects their probability as a function of delay  $\tau = t_{\text{start}}(XX) - t_{\text{stop}}(X)$ . As one expects an enhanced probability to find an X photon at

short time scales after an XX decay but *not* for the inversed scenario, the fingerprint of such a photon cascade should be a significant correlation trace asymmetry of anti-bunching (suppressed signal) and bunching (increased signal; see sketched trace in (03b) in the vicinity of zero delay. This behaviour is indeed observable under the conditions of continuous wave optical excitation, as will be discussed in detail in the following paragraphs.

#### 4. Efficient generation of triggered single photons and photon pairs

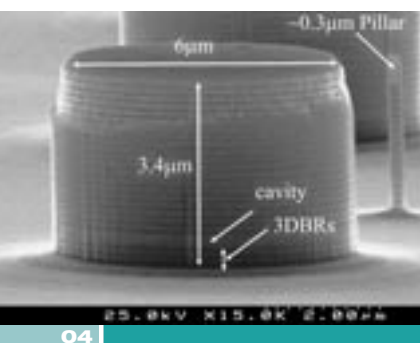
With respect to future applications in the fields of quantum information technology, there is an important requirement to be fulfilled for an effective use of single-photon emitters: As the spontaneous emission of photons is randomly distributed over the full solid angle  $4\pi$  of space and is therefore subject to photon losses by total internal reflections on the semiconductor-vacuum surface, this reduces the photon-capture efficiency for any optically coupled devices (e.g., fibers for collection of the emission). It is therefore desirable to channel the stream of emitted photons which can be achieved by embedding QDs into micro-resonator structures. These resonator structures are characterized by well defined spectral and spatial mode profiles as a consequence of a strong lateral and vertical confinement of the light field.

The use of semiconductor microcavities leads to a drastic increase of the light emission efficiency of devices. A vertical pillar microcavity is formed by a pair of bottom/top distributed-Bragg reflectors (DBRs) separated by a cavity region containing an active material layer in the center. Inside the  $\lambda$ -cavity the optical field is trap-

#### ZUSAMMENFASSUNG

*Die gezielte Ausnutzung der quantenmechanischen Eigenschaften von Licht (Photonen), welche insbesondere auf Basis von Halbleiter-Nanostrukturen erzeugt werden, eröffnet zahlreiche neue Möglichkeiten für Anwendungen auf dem Gebiet der Photonik bzw. Quanten-Informationstechnologie. Dazu zählen insbesondere die Entwicklung abhörsicherer Datennetze sowie verschiedene Konzepte für das optische Quantencomputing. Weitere viel versprechende Einsatzgebiete ergeben sich im Bereich der bildgebenden Verfahren (Imaging) sowie der Mikrostrukturierung (Lithographie) durch die Möglichkeit, eine Auflösungsgrenze unterhalb des beugungsbedingten Limits zu erreichen. Grundvoraussetzung für eine Vielzahl derartiger Anwendungen ist die Verfügbarkeit von deterministischen Photonquellen, welche in der Lage sind, “Einzelphotonen auf Bestellung” zu erzeugen. Einzelne Halbleiter-Quantenpunkte in Mikroresonatoren eröffnen diese Möglichkeit, wobei ultra-hohe Wiederholraten von bis zu 1 GHz erreicht werden.*

*Dieses Kapitel gibt einen Einblick in die spannende Physik von Halbleiter-Nanostrukturen, insbesondere ihre Anwendung als nicht-klassische Lichtquellen. Basierend auf Quantenpunkten, eingebettet in eine Mikroresonator-Struktur, wird die effiziente Erzeugung einzelner Photonen sowie von Photonenpaaren demonstriert. In diesem Zusammenhang sollen ebenfalls die augenblicklichen physikalischen Grenzen dieser Technologie diskutiert werden.*



04

Scanning-electron microscope (SEM) micrograph of AlAs/GaAs pillars fabricated by electron beam lithography and dry etching.

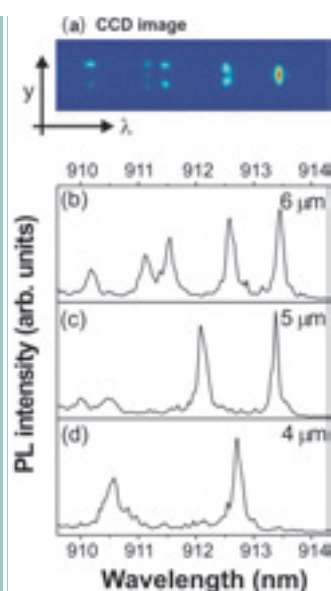
ped, where  $\lambda/n$  is the wavelength of the light in the material. The DBRs are formed by alternating epitaxial growth of  $\lambda/4n$  layers of semiconductor or dielectric materials of different refractive indices. As DBR semiconductor materials being lattice matched to the substrate material typically have a small refractive index contrast (e.g.,  $n_{\text{AlAs}} = 2.92$  and  $n_{\text{GaAs}} = 3.52$ ), several mirror periods are required to reach a sufficient reflectivity of more than 99.9 percent. The almost total internal reflection in the microcavity leads to the formation of cavity modes. By embedding QDs as the active layer in semiconductor microcavities, one can (a) guide the light emission in a desired direction, (b) control the emission wavelength and (c) also the emission patterns. In practice, the emission energy of a QD should be in resonance with the mode of the microcavity to achieve high collection efficiency. In this study, 23- and 20-period bottom and top DBRs of AlAs/GaAs layers, respectively, were used. Each DBR period consists of a 79 nm AlAs/67 nm GaAs layer pair. A 1.4 nm thick single layer of self-assembled QDs is used as the active region at the centre of a GaAs cavity. (04) illustrates a scanning electron microscope (SEM) micrograph of such typical AlAs/GaAs microcavity pillars [2].

In this picture two different pillar sizes are visible. The larger structure has a nominal diameter of 6  $\mu\text{m}$  and the smaller one has a diameter of 0.3  $\mu\text{m}$  with a height of 3.4

$\mu\text{m}$  (only three layers of the bottom DBR have been etched away). The pillar sidewalls are nearly vertical with only small damages appearing next to the top surface.

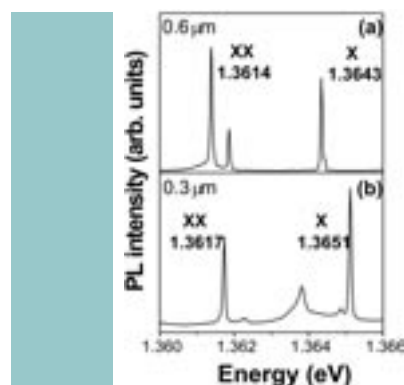
To characterize the investigated system, photoluminescence emission spectra of (In,Ga)As QDs in pillar microcavities of decreasing diameter have been studied. Since larger-diameter pillars typically contain a huge number of QDs, the inhomogeneously broadened ensemble PL (due to the QD size distribution) can be used as an internal light source to reveal the pillar mode structure. For instance, the charge-coupled device (CCD) image in (05a) provides a one-dimensional cross section through the emitted intensity pattern of the 6  $\mu\text{m}$  pillar in the plane parallel to the mirror layers as a function of the emission wavelength. This CCD image experimentally accesses the transverse mode structure: the outermost right peak is identified as the fundamental mode (having a field maximum in the center and a simple Gaussian-like shape); other peaks correspond to higher-order modes. A quality factor  $Q$  ( $\lambda/\Delta\lambda$ ) of  $\sim 10\,000$  is estimated for the fundamental mode. (05b), (05c) and (05d) display the measured PL spectra of 6, 5 and 4  $\mu\text{m}$  diameter pillars, respectively. For decreasing pillar diameter, these spectra show characteristic properties: (i) The wavelength of the fundamental mode decreases with diameter ( $D$ ) and (ii) the spacing between resonant wavelengths increases monotonically for decreasing diameter (approximately as  $D^{-2}$ ).

To access individual QD emission, PL measurements were performed on small diameter pillars. Since a single layer of QDs is positioned between the cavity mirrors, microstructuring with decreasing circular pillar cross section cuts out an area with a reduced number of QDs. For a diameter of 0.3  $\mu\text{m}$  the pillars contain about 21 QDs and since the linewidth of the QD ensemble is considerably larger than the linewidth of a mode, only very few QDs will therefore fit energetically to a certain cavity mode. As a consequence, the emission spectra of (06a) and (06b) do not reflect the cavity mode structure but sharp emission lines of individual QDs. From our mode calculations (not shown here) we conclude that the observed lines shown in the respective figures appear within the same cavity mode.



05

(a): Spectrally resolved charge-coupled device image as a cross-section of the 6  $\mu\text{m}$  pillar mode structures; (b), (c), and (d): measured cavity spectra for decreasing pillar diameters of 6, 5 and 4  $\mu\text{m}$ , respectively.



06

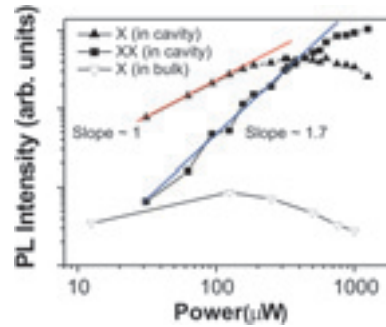
Photoluminescence spectra from pillars with diameters of (a) 0.6  $\mu\text{m}$  and (b) 0.3  $\mu\text{m}$  observed under pulsed laser excitation.

In each case the spectra are dominated by a pair of PL lines which were assigned to excitonic ( $X$ ) [1.3643 eV (a) / 1.3651 eV (b)] and biexcitonic ( $XX$ ) emission [1.3614 eV (a) / 1.3617 eV (b)] due to their linear and superlinear dependence on excitation power, respectively. As will be shown in the following, in either case these line pairs originate from the same single quantum dot. The appearance of additional PL lines between  $X$  and  $XX$  is not fully clarified, but could result from a charged exciton transition of the same QD or a further excitonic transition from a different QD.

**(07)** shows the cw laser power dependence of the  $X$  (closed triangles) and the  $XX$  (squares) intensities from the 0.6  $\mu\text{m}$  pillar microcavity as well as, for comparison, the typical  $X$  (open triangles) intensity observed from a QD in a bulk semiconductor. The  $X$  line in the pillar cavity shows an approximately linear power dependence, therefore reflecting a QD configuration containing only a single photo-excited electron-hole pair. In contrast to this, the  $XX$  line reveals a superlinear increase with a slope of 1.7 which is attributed to emission from the QD containing two photo-excited electron-hole pairs. At high cw excitation powers a saturation behaviour is observed for both lines. An enhancement of the PL intensity by a factor of  $\sim 40$  was found for  $X$  in a pillar microcavity when compared to the PL intensity of  $X$  in bulk semiconductor. The following two effects contribute to this observation: (1) the exciton transition being mainly coupled into the cavity mode by the Purcell effect and/or (2) the enhanced photon collection efficiency due to channeled emission out of the cavity structure. The enhancement of the spontaneous emission rate in the cavity resonance is given by the Purcell factor which is proportional to the Q-factor of the mode and inversely proportional to the mode volume. Purcell factors up to 10 have already been realised in QD pillar cavities. Due to this cavity effect, the lifetime of the photon emission is dramatically reduced with respect to its value in bulk semiconductors, hence also allowing high repetition rates ( $\sim 1$  GHz) of these kinds of single photon sources.

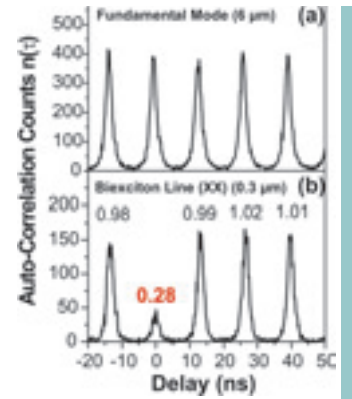
Autocorrelation measurements have been performed to demonstrate single-photon generation under pulsed excitation of QDs in pillar microcavities with different pillar diameters. For instance, **(08)** shows the

measured unnormalized correlation function  $n(\tau)$  of the fundamental mode of the 6  $\mu\text{m}$  pillar **(08a)** and of the  $XX$  QD emission from the 0.3  $\mu\text{m}$  pillar **(08b)**. The corresponding PL spectra are given in **(05b)** and **(06b)**, respectively. The mea-



07

Continuous-wave laser power dependence of the  $X$  (closed triangles) and  $XX$  (squares) intensities from a QD located in a 0.6  $\mu\text{m}$  diameter pillar microcavity in comparison to excitonic emission from a QD in a bulk semiconductor (open triangles).



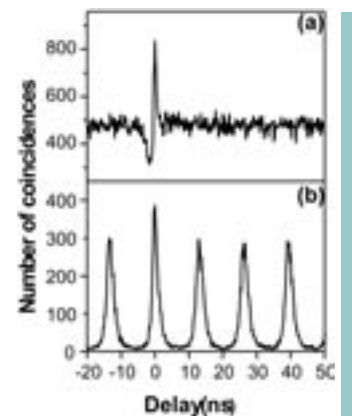
08

Autocorrelation measurements under pulsed laser excitation obtained from (a) a fundamental mode of a 6  $\mu\text{m}$  diameter pillar (PL spectrum in **(05b)**) and (b) the  $XX$  photon of a 0.3  $\mu\text{m}$  diameter pillar (PL spectrum in **(06b)**).

sured  $n(\tau)$  of both pillars exhibit peaks at integer multiples of the laser pulse repetition period  $T_{\text{rep}} = 13.12$  ns, indicating a locking of the photon emission to the pulsed excitation. The correlation peak areas are related to the conditional probability to detect a second photon (on the stop) after the first photon has already been detected during the excitation cycle. As expected, for the 6  $\mu\text{m}$  pillar diameter all correlation peaks have the same areas which is expected for a Poissonian light source.

This is due to the fact that many QDs contribute independently to the mode emission. In contrast to the 6  $\mu\text{m}$  pillar, the central peak at  $\tau = 0$  ns of the 0.3  $\mu\text{m}$  pillar is significantly suppressed, demonstrating the single-photon nature of the emitted light. However, for a perfect single-photon emitter one expects  $g^{(2)}(0) = 0$ . For the 0.3  $\mu\text{m}$  pillar,  $g^{(2)}(0) = 0.28$  is observed for the central correlation peak which does not reach its theoretical value of zero. This is attributed to the presence of a weak uncorrelated background originating mainly from the wetting layer and leaky modes.

In order to prove the cascaded nature of  $XX$  and  $X$  emission, cross-correlation mea-



09

Cross-correlation measurements of  $X$  (stop) and  $XX$  (start) photons from a 0.6  $\mu\text{m}$  diameter pillar recorded under (a) cw laser excitation and (b) pulsed excitation, respectively.

## THE AUTHORS

**DR. MOHAMED BENYOUCEF (L.)**

received his Ph.D. degree from the department of physics, University of Bristol (UK) in February 2002. Having worked as a research associate at the Institute of Solid State Physics (University of Bremen) and the 5<sup>th</sup> Institute of Physics (University of Stuttgart), he started in August 2005 in the MBE group at the Max-Planck-Institute for solid state research, Stuttgart. His current research interests include self-assembled quantum dots, quantum dots in microcavities, microcavity lasers, semiconductor nanostructures, and development of single photon sources.

**PROF. DR. PETER MICHLER (M.)**

is the head of the department “Neue optische Materialien und Technologien” at the 5<sup>th</sup> Physics Institute of the Universität Stuttgart. His group studies the fundamental electronic and quantum optical properties of semiconductor nanostructures with respect to applications in photonics and quantum information technology.

**SVEN MARCUS ULRICH (R.)**

studied physics at the University of Bremen (Germany) where he received his diploma degree on “Optical Spectroscopy of Donor-Acceptor Pair Recombinations in GaN:Mg” in 2001. His current Ph.D. work as a scientist at the 5<sup>th</sup> Institute of Physics (Universität Stuttgart) focuses on the generation of non-classical light states from individual semiconductors quantum dots, with particular interest in single and cascaded photons, as well as QDs in microcavity laser structures.

**Contact**

5. Physikalisches Institut, Universität Stuttgart, Pfaffenwaldring 57, 70550 Stuttgart

Tel. +49 (0)711 685 4660

Fax +49 (0)711 685 3810

E-mail: p.michler@physik.uni-stuttgart.de

measurements were performed on the 0.6  $\mu\text{m}$  diameter pillar. The PL spectrum is depicted in (06a). (09a) shows the cross correlation measured by using the XX transition to trigger the start channel and the X to supply the stop, recorded under cw laser excitation. The cross correlation reveals asymmetric features, i.e., bunching ( $\tau > 0$ ) and antibunching ( $\tau < 0$ ) due to cascaded emission. In detail, there is a suppressed probability to detect an exciton photon before the biexciton which leads to the observed antibunching behaviour. The dip in the cross correlation in the vicinity of  $\tau = 0$  again does not reach its theoretical value of zero due to the presence of an uncorrelated background. For  $\tau > 0$  the enhanced probability to observe an X decay following an XX photon gives rise to the bunching behaviour. We have repeated the same cross-correlation experiments under pulsed excitation, the histogram of

which is shown in (09b). Again the cross-correlation displays a series of peaks separated by the laser period of 13.12 ns. The zero delay peak integral appears larger than the other peaks (“bunching”), which again reflects the cascaded nature of subsequent X photon-XX photon decay processes. This bunching effect is the signature for the generation of triggered photon pairs. Note that similar results were found for the 0.3  $\mu\text{m}$  diameter pillar.

In conclusion, we have demonstrated the possibility of using the biexciton-exciton radiative cascade of a single quantum dot (QD) in a pillar microcavity to efficiently generate triggered photon pairs. Due to the enhanced photon collection efficiency out of the cavity structure an increase of the photoluminescence intensity by a factor of  $\sim 40$  was found as compared to the corresponding QD PL intensity in bulk semiconductor material.

## 5. Outlook

The presented experimental results have demonstrated the high potential of semiconductor nanostructures for the realization of single-photon sources and photon pair emitters. However, a few technological challenges remain for practical devices. The currently investigated QDs emit in the near infrared spectral region ( $0.85\ \mu\text{m} - 1\ \mu\text{m}$ ) and possess shallow electronic confinement potentials which prevents a high quantum efficiency of the emission at temperatures above  $\sim 50\ \text{K}$ . CdSe/Zn(S,Se) or (In,GaN)/GaN QDs with higher electronic confinement potentials and higher bi-exciton binding energies may provide a solution for room temperature operation in the blue-green spectral region. Promising results from CdSe/Zn(S,Se) QDs have been recently reported by us [1]. We observed the generation of triggered single-photons with epitaxially grown self-assembled CdSe/Zn(S,Se) QDs for temperatures up to 200 K. For fiber-optical communications one would prefer to use the dispersion and absorption minima of the optical fiber at  $\sim 1.3\ \mu\text{m}$  and  $\sim 1.55\ \mu\text{m}$ , respectively.

Very recently, first results for the  $1.3\ \mu\text{m}$  telecom fiber range have been reported from the group of A. Shields from Toshiba [3]. They reported on-demand single photon emission from a microcavity sample with a low density of large InAs/GaAs self-assembled quantum dots into the fiber-optic transmission band at  $1.3\ \mu\text{m}$ .

A precondition for mass production of devices is the *controlled* coupling of the QD emission to a cavity mode with directional field profile in order to achieve a high photon collection efficiency. For this task the spatial position of the QD and the energy of its transition has to be adjusted with respect to the maximum of the mode profile and the energy of the cavity mode, respectively. The former task is still a challenge although considerable progress has been made on pre-patterning of MBE samples to create nucleation spots on which QD growth takes place. Together with our colleagues from the Max-Planck-Institut für Festkörperforschung, Stuttgart (Group of O.G. Schmidt), we are planning to tackle this challenging task in the near future. The energetic resonance condition can be achieved by temperature tuning or by electric field tuning via the quantum-confined Stark effect. However, the QD

transition energies are only defined within a relatively broad inhomogeneous linewidth ( $\sim 10 - 30\ \text{meV}$ ) of the corresponding QD ensemble. That implies that several QDs have to be placed inside a cavity so that one can be tuned into resonance. Therefore, control of QD exciton energies during or after growth by e.g., an annealing technique would certainly constitute a breakthrough for numerous applications.

In summary, the ongoing progress on the fabrication procedure of pillar cavities and quantum dots opens the way to highly-efficient single-photon sources and new types of applications in the field of quantum information technology. •

Mohamed Benyoucef  
Sven Marcus Ulrich  
Peter Michler

## References

- 1 K. Sebald *et al.*, Appl. Phys. Lett. **81**, 16, 2920 (2002).
- 2 M. Benyoucef *et al.*, New Journal of Physics **6**, 91 (2004).
- 3 M. B. Ward *et al.*, Appl. Phys. Lett. **86**, 201111 (2005).